Tech Science Press

Ecofriendly E-Nose Based in PLA and Only 0.3 wt% of CNTs

Laura Ribba, Jonathan Cimadoro and Silvia Goyanes*

Universidad de Buenos Aires, Facultad de Ciencias Exactas y Naturales, Departamento de Física, Laboratorio de Polímeros y Materiales Compuestos (LP&MC), Instituto de Física de Buenos Aires (IFIBA-CONICET), Ciudad Universitaria (1428), Ciudad Autónoma de Buenos Aires, Argentina.

*Corresponding Author: Silvia Goyanes. Email: goyanes@df.uba.ar.

Abstract: In this work, conductive polymer nanocomposites were developed based on a biodegradable and biobased polymer (poly (lactic acid)), with the incorporation of only 0.3 wt% of carbon nanotubes (CNTs) to be used as volatile solvent sensors. The correct dispersion of the nanofiller was achieved thanks to a CNT non-covalent modification with an azo-dye (disperse orange 3) which allowed to reach the percolation for electric conduction in values as low as 0.3 wt%. The chemo-resistive properties of the developed sensors were investigated by exposure to organic vapors (ethanol, tetrahydrofuran and toluene) and water vapor, showing good selectivity. In addition, considering the manipulation to which the sensor will be exposed, wear resistance was characterized, finding that the incorporation of CNTs produced an increase in more than a 50%.

Keywords: Poly (lactic acid); carbon nanotubes; sensor; CPC; organic solvent vapor; DO3

1 Introduction

Conductive polymeric composites (CPC) are intelligent materials obtained through the incorporation of conductive nanoparticles within matrices of insulating polymers. Nowadays the lifetime of materials in general, and in particular of electronic products, is getting shorter. This poses a growing ecological problem due to the accumulation of waste. Biodegradable intelligent products have great potential to reduce the environmental footprint of devices. Through the use of biodegradable polymers in the development of CPC, complex green electronic components can be developed [1,2].

Poly (lactic acid) (PLA) is a biodegradable thermoplastic polymer, which has large stiffness, high tensile strength, good film-forming properties and gas permeability [3]. Different CPCs based on PLA have been proposed in literature, incorporating several conductive fillers such as carbon nanotubes (CNT) [4], graphene [5] and silver nanoparticles [6]. In particular, due to their good electrical conductivity, high aspect ratio and the quantum effects connected to their nanometric structure, CNTs have been investigated as sensitive materials [7]. The operation principle of these sensors is based on changes in their conductivity as a result of adsorption of specific molecules on their surface. The interaction of CNTs with functional groups (including carboxyl and amino groups), metallic nanoparticles and polymers lead to the formation of chemically active sensors [8]. This type of sensors has been applied to detect small concentrations of volatiles in the air [4,7,8]. In particular, Wei et al. [4] show the application of a PLA and CNTs sensor to detect with high resolution, 50 ppm of chloroform. It is extremely important to maximize the matrix-nanotube interface area in order to develop this application. The dispersion of the filler is then a critical aspect of the nanocomposite manufacturing method. However, the inherent difficulty to obtain proper CNTs dispersions requires the incorporation of a larger amount of nanotubes to reach the conduction thresholds [9,10].

Several authors have studied polymer-CNTs nanocomposites [4,7,11,12,13]. In order to improve the filler's dispersion, different physical and chemical modifications were performed; from the realization of

covalent and non-covalent functionalizations through electrostatic interactions, to modifications in the applied shear stress during the dispersion processes, or the inclusion of different additives [14,15,16,17].

Some of these processes can introduce defects on the nanotubes walls or even decrease their aspect ratio and therefore worsen their important properties. For example, it has been reported that after a carboxylation treatment of CNTs, their sidewall began to be destroyed up to their nearly complete destruction [18]. One way to improve its dispersion, without substantially affecting its characteristics, is through non-covalent functionalization. In particular, it has been demonstrated that a molecule of azo dye, Disperse Orange 3 (DO3), can efficiently improve the dispersion of CNTs in an organic solvent, tetrahydrofuran (THF), without damaging its molecular characteristics and thus preserving its properties [12]. Moreover, using this methodology PLA-CNTs with important improvements in ductility have been successfully developed [15].

The objective of this work is to develop a poly (lactic acid) CPC to be applied as a volatile solvent sensor using sufficiently low amounts of additives to avoid altering the ecological character of the material. In particular, 0.30% by weight of CNTs and 0.25% by weight of DO3 was used. Sensing properties of the nanocomposites were characterized, showing the great potential of this material in the field of smart packaging. Besides, the wear of nanocomposites was studied in order to have an idea of the response to friction with different objects that could wear out the packaging and act on the sensor.

2 Methods

Materials were developed from PLA (10% D-Lactide, 90% L-Lactide) with 67.600 $g.mol^{-1}$ and 49.900 $g.mol^{-1}$ weight and number averaged molecular weight respectively (Shenzhen Bright China Industrial Co. Ltd), DO3 dye (Sigma-Aldrich), CNTs (Nanocyl, NC3100) and reagent grade chloroform (Biopack, Argentina).

The nanocomposites were prepared using three different concentrations of CNTs: 0.05 wt%, 0.1 wt% and 0.3 wt%, following the procedure previously reported by our group [15]. Basically, 0.0005, 0.0010 or 0.0030 g of CNTs were dispersed, depending on the desired concentration, together with 0.0025 g of DO3 in 50 ml of chloroform by ultrasound for 90 minutes. Next, 1 g of PLA was added and the mixture was exposed to ultrasound for further 60 minutes. The resulting solution was cast into Petri dishes and the solvent was allowed to evaporate at room temperature for 24 h. The drying process continued in a vacuum oven at 40ºC during four days and a final stage of 24 hours at 60ºC, always under vacuum. The complete removal of residual solvent was confirmed by NMR analysis. Films of PLA and PLA-DO3 were prepared in the same way as the nanocomposites for comparison purposes. Five different films of each kind of sample were prepared. The mean thickness of each set of five samples was 75 μm with a dispersion of 2 μm. It should be emphasized that for all CNTs concentrations the same amount of DO3 was used, since in a previous work [15], it was demonstrated that the inclusion of DO3 in PLA modifies both its mechanical properties and its crystallinity. Then in order to keep the same matrix material, it was decided to use a fixed DO3 concentration. The 0.3 wt% value respect to PLA was chosen as it leads to good nanotubes dispersion for the maximum amount of filler used [19].

The dispersion of CNTs in the nanocomposite was studied by scanning electron microscopy (FE-SEM) of the cryogenic fracture surfaces using a Zeiss DSM982 GEMINI equipment operated at 20 kV.

The electrical response of the nanocomposites was studied by recording their resistance when exposed to successive cycles of dry nitrogen and vapor currents of different solvents at 23ºC. Three different cycle times of exposition at solvent vapors were studied, 10 minutes, 20 minutes and 30 minutes. In all cases the reversibility study was repeated for three cycles. Solvents used for this work were water, ethanol, tetrahydrofuran and toluene. The system used to carry out the measurements consisted of flow controllers, bubblers and a chamber where the sample was placed, as it is shown in Fig. 1(b). Bubbling dry nitrogen in liquid solvent provides a saturated vapor stream (100% vapor concentration). nAll the experiments were carried at a constant flow (Qv = 200 cm^3min^{-1}). The electrical resistance of the samples was recorded with a Hewlett Packard multimeter model 34401A. In order to improve the electrical

contact between the alligator clips of the multimeter and the film, electrodes were generated on both sides of the sample depositing a thin layer of gold using plasma methods (sputtering) as it is shown in Fig. 1(a). Multimeter alligator clips were attached directly to those electrodes. The resistance (R) was measured three times on three different samples of each nanocomposite and the electrical resistivity (ρ) was calculated by equation:

$$\rho = R.\frac{A}{L} \tag{1}$$

where A is cross section of the sample and L is its length. The volumetric electrical conductivity (σ) was calculated as the inverse of the electrical resistivity.

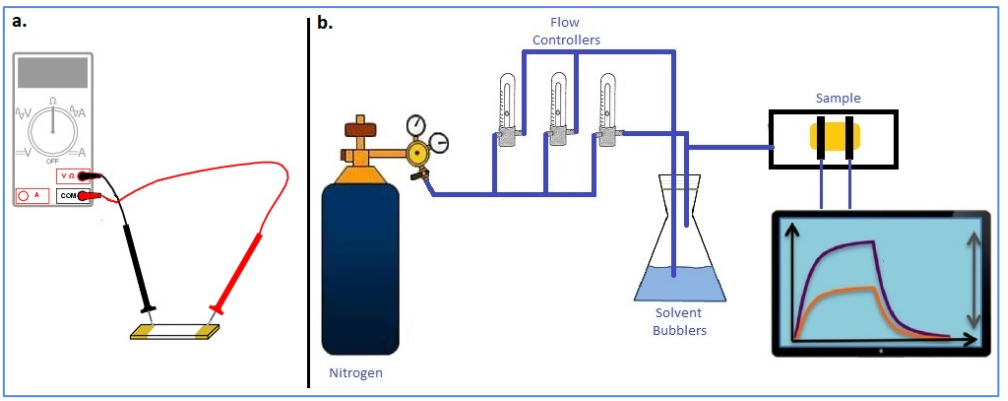

Figure 1: a. Scheme of electrical resistance measurement. **b.** Scheme of vapor sensing device

The relative resistance amplitude value (Ar) was calculated from the resistance values measured by the equation:

$$A_r(t) = \frac{R(t) - R_0}{R_0} \tag{2}$$

where R represents the resistance of the nanocomposite at time t and R_0 the initial resistance when exposed to the flow of dry nitrogen.

The wear of the developed materials was measured with a Calotest device [20] developed in our laboratory. The volume displaced by a stainless steel sphere that rotates on the material was calculated from the diameter of the mark produced. Using the Archard model, the sliding wear coefficient was determined according to the equation:

$$V = k \cdot S \cdot N \tag{3}$$

where k represents the wear coefficient, V the wear volume, S the displaced distance and N the normal applied force. The tests were repeated five times for each type of material. It should be noted that these measurements were carried out before exposing the samples to the different solvents.

In order to study the existence and size of crystallites in the different samples, a study via crossed polarizing microscopy was performed using a Zeiss Axioplan microscope (plan apochromat objectives) and Nomarski polarizers (DIC-differential interference contrast). Due to the optical birefringence of the crystallites, crystalline zones should appear with different colors in the microscope micrographs.

3 Results and Discussion

Fig. 2 shows FE-SEM micrographs of the cryogenic fracture surface of a sample of PLA-DO3-CNTs 0.3 wt%. It is possible to observe a good degree of dispersion of nanotubes in the matrix.

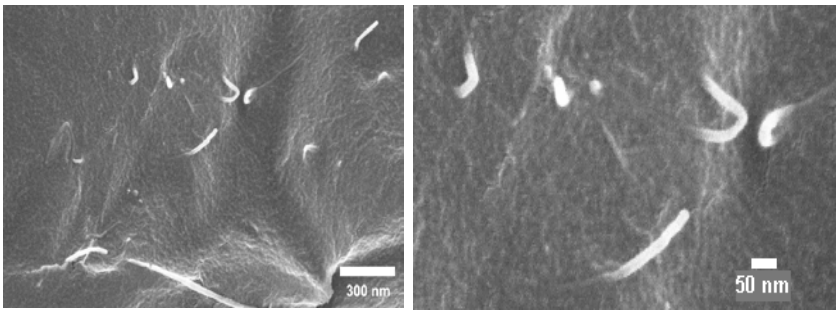

Figure 2: FE-SEM micrographs of the cryogenic fracture surface of nanocomposite PLA-DO3-CNTs 0.3 wt%

Conductivity values obtained for the different materials are listed in Tab. 1. All PLA-DO3-CNTs nanocomposites showed an improvement in electrical conductivity compared to pure PLA and PLA-DO3. The conductivity of PLA and PLA-DO3 were of the same order. Although the addition of 0.05 wt% and 0.1 wt% of CNTs improved the conductivity of PLA in two orders of magnitude, the nanocomposite with 0.3 wt% of CNTs presents a conductivity ten orders of magnitude larger than neat PLA.

Different reports in literature indicate that the percolation threshold for PLA-CNTs nanocomposites occurs with conductivity values ranging from 10^{-3} S m^{-1} to 10^{-5} S m^{-1}. [7,17,21] Although in our work the percolation threshold was not determined, the conductivity of the sample with 0.3 wt% of CNTs (1.6×10^{-1} S m^{-1}) is much higher than those reported in percolation, indicating that our system is percolated and that we are working at a CNTs concentration much higher than that needed for percolation.

Table 1: Conductivity values of the studied materials

Material	Conductivity (S m^{-1})
PLA	$(3 \pm 1) \times 10^{-11}$
PLA-DO3	$(5 \pm 1) \times 10^{-11}$
PLA-DO3-CNTs 0.05 wt%	$(7 \pm 1) \times 10^{-9}$
PLA-DO3-CNTs 0.1 wt%	$(5 \pm 1) \times 10^{-8}$
PLA-DO3-CNTs 0.3 wt%	$(1.6 \pm 0.5) \times 10^{-1}$

Based in these results the nanocomposite with 0.3 wt% of CNTs was chosen to be studied as a vapors sensor. It was found that each solvent has its own impact on the variation of the resistance, an extremely useful effect for the detection and identification of gases [10,22]. The relative resistance amplitude of the sample as a function of time when exposed to periodic successive cycles of 10 minutes of dry nitrogen and vapor currents of different solvents at 23ºC can be seen in Fig. 3.

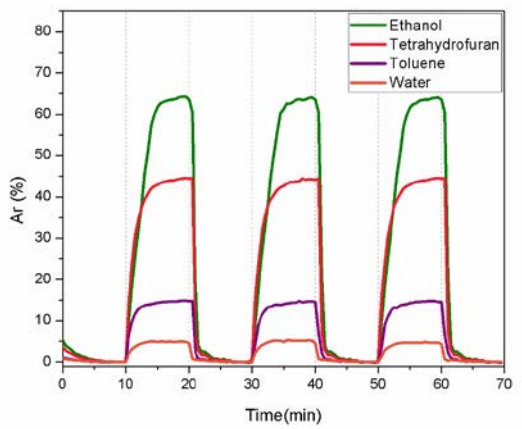

Figure 3: Amplitude of relative resistance (Ar) of the material as a function of time when exposed to 10-minutes cycles of dry nitrogen and vapor currents from different solvents

From curves presented in Fig. 3, it can be seen that the reversibility of the material is complete upon completion of each 10-minute cycle. For the other cycle times of exposition at solvent vapors the obtained results were analogue, showing a complete material reversibility. It is also observed that the greatest difference in resistance was obtained for ethanol, while the lowest difference was for water vapor.

The sensitivity to the different solvents is defined as the highest Ar value reached for each solvent. Values found are shown in Tab. 2.

Table 2: Sensitivity values found for each solvent

Solvent	Sensitivity
Ethanol	64,3 ± 0,1
Tetrahydrofuran	44,4 ± 0,1
Toluene	14,8 ± 0,1
Water	4,9 ± 0,1

The selectivity of the sensors is a very important point, since it would reduce the number of sensors necessary for the identification of molecules in an electronic nose.

It is known that the swelling of polymer matrices originated from the absorption and diffusion of good solvents, could lead to the disconnection of the conductive pathways at different degrees and increase in resistance [4]. While this effect should be notorious near the percolation threshold, in our case being well above it (3 orders of magnitude in conductivity), this effect should be minimal, at least in the timeslots and number of repetitions studied. For that reason, a specific study of this phenomenon was not carried out, but it should be kept in mind if the material would be employed for longer periods than those studied in this work.On the other hand, the wear coefficient (K) was determined for all materials using the Archard model [20], as one of the necessary characteristics of the sensor's material is that it is resistant to the wear produced by manipulation. From Fig. 4, it can be seen that the addition DO3 increases the wear coefficient showing that the film with DO3 wears more easily than that of neat PLA. With an addition of 0.05 wt% and 0.1 wt% of CNTs, the wear coefficient does not show significant changes compared to the one of PLA-DO3. However, with increasing concentrations of the nanotubes, this effect is reversed. The addition of 0.3 wt% of CNTs leads to a strong decrease in the wear coefficient, indicating an increase of more than a 50% in wear resistance.

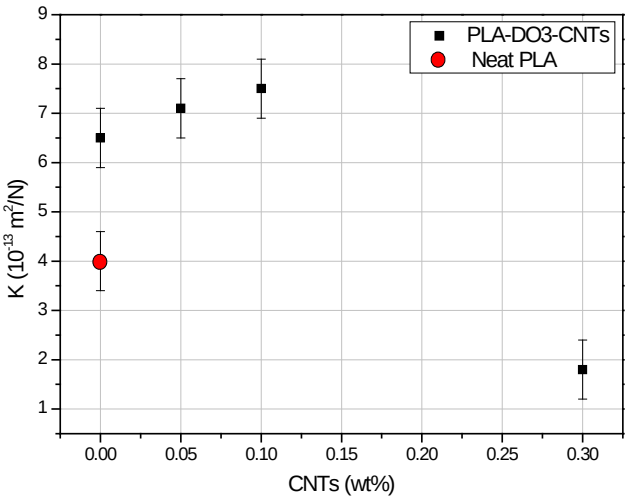

Figure 4: Wear coefficient for all developed materials

Different mechanisms could produce changes in tribological behaviors of polymeric nanocomposites, such as changes in morphology of the polymer (molecular weight, crosslink density for thermosets, crystallinity for semi-crystalline polymers), and a direct effect of nanoparticles on the wear mechanism (e.g., improved adhesion of the transfer film) [23]. In general higher crystallinity leads to higher wear resistance [24]. However, if crystal domain sizes differ, this relation is more complex.

In a first approximation, crystalline domains could be thought of as a rigid filler with respect to the matrix material. In a composite material with microfillers the wear decreases if these can be easily deformed, while if they do not it trends to increase [25] In a general sense, the interactions among the elements of the sliding systems are believed to affect the wear process [26]. That is, during the wear process, the interface between the two materials as well as the difference between the ability to deform of each one is what determines the result [25,26]. On the other hand, in the case of nanometric fillers several authors have shown that a low friction and high wear resistance is obtained since the size of nanoadditives is of the order of surrounding polymer chains what increases bonding of particles to the polymer matrix [24,27,28]. Also, the nanosized filler tends to produce a tenacious transfer on the counterface, which protects the composite surface from direct contact with the counterface and reduces the friction and wear of nanocomposites.

A first way to study the crystallinity of samples would be by X-ray diffraction. In a previous work of the group it was demonstrated that PLA films had two very small diffraction peaks that correspond to both, the α and the β crystal structures characteristics of this polymer. In contrast, the diffraction pattern for the PLA-DO3 film showed more clearly defined diffraction peaks, indicating a greater degree of crystallinity, which corresponded only to the α-form [15]. When only 0.05 wt% CNTs content was added together with DO3, the β-form is again observed ($2\theta = 30.9^{o}$), and the pattern shows a strong increase of crystallinity compared to neat PLA, but less crystallinity than PLA-DO3 samples. Although the results reported corresponded to the sample with the lowest CNTs concentration, analogous results were obtained for the concentration of 0.3 wt%.

In order to study the formation of crystalline structures (crystallities), polarized light microscopy was used. Micrographs obtained for PLA, PLA-DO3 and PLA-DO3-CNTs 0.3 wt% are shown in Fig. 5. Films of PLA with DO3 showed crystallities of approximately 1 μm, while films of neat PLA did not. This difference in the crystalline structure of materials is a possible explanation for the fact that the material made from PLA and DO3 has a lower wear resistance than neat PLA. The material with DO3 shows small crystalline zones surrounded by big amorphous areas. The outer layer of the film could then be worn through these amorphous areas easily than the PLA matrix.

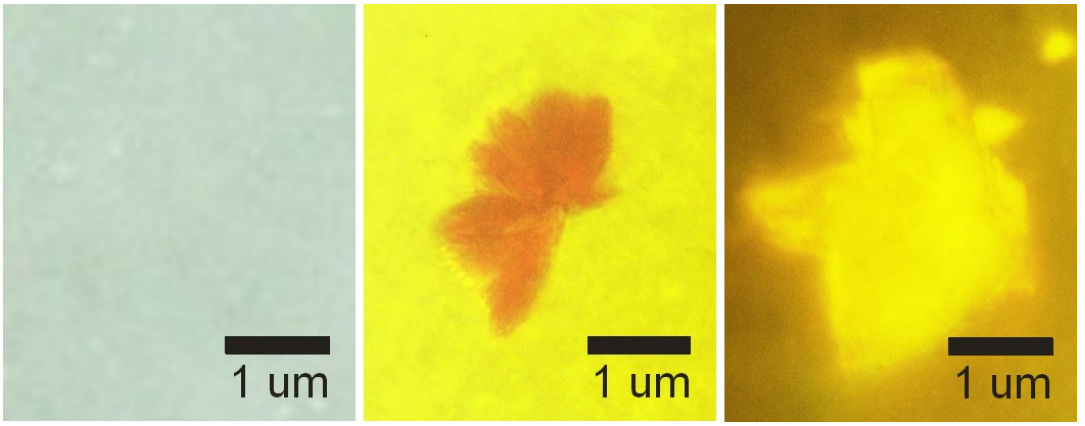

Figure 5: Polarized light micrographs of PLA, PLA-DO3 and PLA-DO3-CNTs 0.3 wt%

With the addition of CNTs these crystallites can still be seen for all filler contents (0.05 wt%, 0.1 wt% and 0.3 wt%). The improvement in wear resistance achieved with 0.3 wt% of CNTs is probably a consequence of an anchoring effect produced by the filler. Zhang et al. [29] suggested that, when CNTs are exposed to the sliding interface, substantial CNTs deformation and fragmentation can occur resulting in a protective effect on the polymeric matrix wear behavior.

4 Conclusions

A new CPC was developed in more than 99% from a biodegradable biobased polymer, capable of detecting the presence of vapors of different organic solvents. For this, the concentration of percolating CNTs in the matrix was studied and it was found to be 0.3 wt%. The order of selectivity of the material was found to be Ar (ethanol) > Ar (THF) > Ar (toluene) > Ar (water), and the sensitivities varied from (64.3 ± 0.1) to (4.9 ± 0.1).

It is noteworthy to mention that only 0.30 wt% of CNTs and 0.25 wt% of DO3 were used for manufacturing the material, achieving the desired sensing properties and an improvement in wear resistance, affecting as little as possible the biodegradable character of the matrix polymer.

Acknowledgments: The authors wish to acknowledge the support and collaboration of: CONICET (PIP 2013-2015 11220120100508CO), UBA (UBACYT 2014-2017: 20020130100495BA; PDTS PX02 2013-2015) and ANPCyT (PICT 2017-2362).

References

1. Muthuraj, R., Sachan, A., Castro, M., Feller, J. F., Seantier, B. et al. (2018). Vapor and pressure sensors based on cellulose nanofibers and carbon nanotubes aerogel with thermoelectric properties. *Journal of Renewable Materials, 6,* 277.
2. Hassan, S. H., Voon, L. H., Velayutham, T. S., Zhai, L., Kim, H. C. et al. (2018). Review of cellulose smart material: biomass conversion process and progress on cellulose-based electroactive paper. *Journal of Renewable Materials, 6,* 1.
3. Auras, R., Lim, L., Selke, S. E. M., Tsuji, T. (2010). *Poly (lactic acid) synthesis, structures, properties, processing, and applications*. John Wiley & Sons, Inc. All, New Jersey.
4. Wei, X. P., Luo, Y. L., Xu, F., Chen, Y. S. (2016). Sensitive conductive polymer composites based on polylactic acid filled with multiwalled carbon nanotubes for chemical vapor sensing. *Synthetic Metals, 215,* 216.

5. Zhuang, Y., Song, W., Ning, G., Sun, X., Sun, Z., et al. (2017). 3D-printing of materials with anisotropic heat distribution using conductive polylactic acid composites. *Materials & Design, 126,* 135.
6. Zhang, K., Yu, H. O., Yu, K. X., Gao, Y., Wang, M. et al. (2018). A facile approach to constructing efficiently segregated conductive networks in poly (lactic acid)/silver nanocomposites via silver plating on microfibers for electromagnetic interference shielding. *Composites Science and Technology, 156,* 136-143.
7. Li, Y., Zheng, Y., Zhan, P., Zheng, G., Dai, K. et al. (2018). Vapor sensing performance as a diagnosis probe to estimate the distribution of multi-walled carbon nanotubes in poly (lactic acid)/polypropylene conductive composites. *Sensors and Actuators B: Chemical, 255,* 2809-2819.
8. Zaporotskova, I. V., Boroznina, N. P., Parkhomenko, Y. N., Kozhitov, L. V. (2016). Carbon nanotubes: sensor properties: a review. *Modern Electronic Materials, 2(4),* 95-105.
9. Castro, M., Kumar, B., Feller, J. F., Haddi, Z., Amari, A. et al. (2011). Novel e-nose for the discrimination of volatile organic biomarkers with an array of carbon nanotubes (CNT) conductive polymer nanocomposites (CPC) sensors. *Sensors and Actuators B: Chemical, 159(1),* 213-219.
10. Kumar, B., Castro, M., Feller, J. F. (2012). Poly (lactic acid)-multi-wall carbon nanotube conductive biopolymer nanocomposite vapour sensors. *Sensors and Actuators B: Chemical, 161(1),* 621-628.
11. Felisberto, M., Arias-Duran, A., Ramos, J. A., Mondragon, I., Candal, R. et al. (2012). Influence of filler alignment in the mechanical and electrical properties of carbon nanotubes/epoxy nanocomposites. *Physica B: Condensed Matter, 407(16),* 3181-3183.
12. Costanzo, G. D., Ribba, L., Goyanes, S., Ledesma, S. (2014). Enhancement of the optical response in a biodegradable polymer/azo-dye film by the addition of carbon nanotubes. *Journal of Physics D: Applied Physics, 47(13),* 135103.
13. Farahani, M. H. D. A., Vatanpour, V. (2019). Polymer/carbon nanotubes mixed matrix membranes for water purification. *Nanoscale Materials in Water Purification,* 87-110.
14. Zheng, X., Huang, Y., Zheng, S., Liu, Z., Yang, M. (2018). Improved dielectric properties of polymer-based composites with carboxylic functionalized multiwalled carbon nanotubes. *Journal of Thermoplastic Composite Materials*.
15. Ribba, L., Goyanes, S. (2016). Improving PLA ductility using only 0.05% of CNTs and 0.25% of an azo-dye. *Materials Letters, 182,* 94-97.
16. Huang, Y. Y., Terentjev, E. M. (2012). Dispersion of carbon nanotubes: mixing, sonication, stabilization, and composite properties. *Polymers, 4(1),* 275-295.
17. Shi, Y. D., Lei, M., Chen, Y. F., Zhang, K., Zeng, J. B. et al. (2017). Ultralow percolation threshold in poly (l-lactide)/poly (ε-caprolactone)/multiwall carbon nanotubes composites with a segregated electrically conductive network. *Journal of Physical Chemistry C, 121(5),* 3087-3098.
18. Goyanes, S., Rubiolo, G. R., Salazar, A., Jimeno, A., Corcuera, M. A. et al. (2007). Carboxylation treatment of multiwalled carbon nanotubes monitored by infrared and ultraviolet spectroscopies and scanning probe microscopy. *Diamond and Related Materials, 16(2),* 412-417.
19. Diaz Costanzo, G., Ledesma, S., Mondragon, I., Goyanes, S. (2010). Stable solutions of multiwalled carbon nanotubes using an azobenzene dye. *Journal of Physical Chemistry C, 114(34),* 14347-14352.
20. Mai, F., Habibi, Y., Raquez, J. M., Dubois, P., Feller, J. F. et al. (2013). Poly (lactic acid)/carbon nanotube nanocomposites with integrated degradation sensing. *Polymer, 54(25),* 6818-6823.
21. Gao, J., Wang, H., Huang, X., Hu, M., Xue, H. et al. (2018). Electrically conductive polymer nanofiber composite with an ultralow percolation threshold for chemical vapour sensing. *Composites Science and Technology, 161,* 135-142.
22. Bhimaraj, P., Burris, D., Sawyer, W. G., Toney, C. G., Siegel, R. W. et al. (2008). Tribological investigation of the effects of particle size, loading and crystallinity on poly (ethylene) terephthalate nanocomposites. *Wear, 264(7-8),* 632-637.
23. Srinath, G., Gnanamoorthy, R. (2007). Sliding wear performance of polyamide 6-clay nanocomposites in water. *Composites Science and Technology, 67(3-4),* 399-405.
24. Friedrich, K., Zhang, Z., Schlarb, A. K. (2005). Effects of various fillers on the sliding wear of polymer composites. *Composites science and technology, 65(15-16),* 2329-2343.

25. Schwartz, C. J., Bahadur, S. (2001). The role of filler deformability, filler-polymer bonding, and counterface material on the tribological behavior of polyphenylene sulfide (PPS). *Wear, 251(1-12),* 1532-1540.
26. Srinath, G., Gnanamoorthy, R. (2005). Effect of nanoclay reinforcement on tensile and tribo behaviour of Nylon 6. *Journal of Materials Science, 40(11),* 2897-2901.
27. Dasari, A., Yu, Z. Z., Mai, Y. W., Hu, G. H., Varlet, J. (2005). Clay exfoliation and organic modification on wear of nylon 6 nanocomposites processed by different routes. *Composites Science and Technology, 65(15-16),* 2314-2328.
28. Zhang, L. C., Zarudi, I., Xiao, K. Q. (2006). Novel behaviour of friction and wear of epoxy composites reinforced by carbon nanotubes. *Wear, 261(7-8),* 806-811.